J|A|C|S
ARTICLES
Published on Web 09/07/2006

When Is Water Not Water? Exploring Water Confined in Large Reverse Micelles Using a Highly Charged Inorganic Molecular Probe

Bharat Baruah, Jennifer M. Roden, Myles Sedgwick, N. Mariano Correa,[†] Debbie C. Crans,* and Nancy E. Levinger*

Contribution from the Department of Chemistry, Colorado State University, Fort Collins, Colorado 80523-1872

Received April 8, 2006; Revised Manuscript Received July 1, 2006; E-mail: debbie.crans@colostate.edu; nancy.levinger@colostate.edu

Abstract: The interior water pool of aerosol OT (AOT) reverse micelles tends toward bulk water properties as the micelle size increases. Thus, deviations from bulk water behavior in large reverse micelles are less expected than in small reverse micelles. Probing the interior water pool of AOT reverse micelles with a highly charged decavanadate (V_{10}) oligomer using ^{51}V NMR spectroscopy shows distinct changes in solute environment. For example, when an acidic stock solution of protonated V_{10} is placed in a reverse micelle, the ^{51}V chemical shifts show that the V_{10} is deprotonated consistent with a decreased proton concentration in the intramicellar water pool. Results indicate that a proton gradient exists inside the reverse micelles, leaving the interior neutral while the interfacial region is acidic.

I. Introduction

A unique microenvironment for carrying out a variety of chemical and biochemical reactions is found in the polar cores of reverse micelles (RMs). RMs have also been used as model systems for studying various reactions in confinement, for example, biological functions, such as enzymatic reactions[1−5] or micellar catalysis.[6−11] Despite their simplicity, they provide an excellent method to study fundamental effects of confinement. The nature of the pH and ionic concentration in the aqueous core of the micelle assumes particular significance for chemical reactions, such as acid-catalyzed reactions,[12,13] electron-transfer reactions,[14−16] and biochemical reactions.[1−5] Thus, studies probing the nature of the water pool in RMs interest both chemists and life scientists.

RMs of sodium bis(2-ethylhexyl) sulfosuccinate (AOT) in nonpolar organic solvent can solubilize water into organized structures containing a water pool surrounded by surfactant polar headgroups. Varying the amount of water ($[H_2O]/[AOT] = w_0$) one can vary the size of water pool.[17] For small RMs, $w_0 < 10$, the physical characteristics of the intramicellar water differ substantially from those of bulk water.[18−24] However, as the water pool grows, the properties of the intramicellar water has been reported to approach the properties of bulk water.[25−33]

[†] Permanent address: Departamento de Química, Universidad Nacional de Río Cuarto, Agencia Postal # 3, C.P. 5800 Río Cuarto, Argentina.

(1) Falcone, R. D.; Biasutti, M. A.; Correa, N. M.; Silber, J. J.; Lissi, E.; Abuin, E. *Langmuir* **2004**, *20*, 5732−5737.
(2) Martinek, K.; Levashov, A. V.; Klyachko, N. L.; Khmelnitski, Y. L.; Berezin, Y. V. *Eur. J. Biochem.* **1986**, *155*, 453−468.
(3) Gebicka, L.; Jurgas-Grudzinska, M. *Z. Naturforsch.* **2004**, *59*, 887−891.
(4) Durfor, C. N.; Bolin, R. J.; Sugasawara, R. J.; Massey, R. J.; Jacobs, J. W.; Schultz, P. G. *J. Am. Chem. Soc.* **1988**, *110*, 8713−8714.
(5) Menger, F. M.; Yamada, K. *J. Am. Chem. Soc.* **1979**, *101*, 6731−6734.
(6) Correa, N. M.; Durantini, E. N.; Silber, J. J. *J. Org. Chem.* **1999**, *64*, 5757−5763.
(7) Correa, N. M.; Durantini, E. N.; Silber, J. J. *J. Org. Chem.* **2000**, *65*, 6427−6433.
(8) Correa, N. M.; Zorzan, D. H.; Chiarini, M.; Cerichelli, G. *J. Org. Chem.* **2004**, *69*, 8224−8230.
(9) Correa, N. M.; Zorzan, D. H.; D'Anteo, L.; Lasta, E.; Chiarini, M.; Cerichelli, G. *J. Org. Chem.* **2004**, *69*, 8231−8238.
(10) Fernandes, M. L. M.; Krieger, N.; Baron, A. M.; Zamora, P. P.; Ramos, L. P.; Mitchell, D. A. *J. Mol. Catal. B: Enzym.* **2004**, *30*, 43−49.
(11) Pal, T.; De, S.; Jana, N. R.; Pradhan, N.; Mandal, R.; Pal, A.; Beezer, A. E.; Mitchell, J. C. *Langmuir* **1998**, *14*, 4724−4730.
(12) Komatsu, T.; Nagayama, K.; Imai, M. *J. Chem. Eng. Jpn.* **2005**, *38*, 450−454.
(13) Boyer, B.; Lamaty, G.; Makhlouf, T.; Roque, J. P. *J. Chim. Phys. Phys.-Chim. Biol.* **1989**, *86*, 2201−2214.
(14) Chakraborty, A.; Seth, D.; Chakrabarty, D.; Hazra, P.; Sarkar, N. *Chem. Phys. Lett.* **2005**, *405*, 18−25.
(15) Borsarelli, C. D.; Cosa, J. J.; Previtali, C. M. *Photochem. Photobiol.* **1998**, *68*, 438−446.
(16) Nandi, N.; Bhattacharyya, K.; Bagchi, B. *Chem. Rev.* **2000**, *100*, 2013−2045.
(17) De, T.; Maitra, A. *Adv. Colloid Interface Sci.* **1995**, *59*, 95−193.
(18) Piletic, I. R.; Tan, H. S.; Fayer, M. D. *J. Phys. Chem. B* **2005**, *109*, 21273−21284.
(19) Tan, H. S.; Piletic, I. R.; Fayer, M. D. *J. Chem. Phys.* **2005**, *122*, 174501/1−174501/9.
(20) Tan, H. S.; Piletic, I. R.; Riter, R. E.; Levinger, N. E.; Fayer, M. D. *Phys. Rev. Lett.* **2005**, *94*, 057405/1−057405/4.
(21) Riter, R. E.; Willard, D. M.; Levinger, N. E. *J. Phys. Chem. B* **1998**, *102*, 2705−2714.
(22) Sando, G. M.; Dahl, K.; Owrutsky, J. C. *J. Phys. Chem. B* **2005**, *109*, 4084−4095.
(23) Abel, S.; Sterpone, F.; Bandyopadhyay, S.; Marchi, M. *J. Phys. Chem. B* **2004**, *108*, 19458−19466.
(24) Faeder, J.; Ladanyi, B. M. *J. Phys. Chem. B* **2000**, *104*, 1033−1046.
(25) Ezrahi, S.; Nir, I.; Aserin, A.; Kozlovich, N.; Feldman, Y.; Garti, N. *J. Dispersion Sci. Technol.* **2002**, *23*, 351−378.
(26) Majhi, P. R.; Moulik, S. P. *J. Phys. Chem. B.* **1999**, *103*, 5977−5983.
(27) Das, S.; Datta, A.; Bhattacharyya, K. *J. Phys. Chem. A* **1997**, *101*, 3299−3304.
(28) Onori, G.; Santucci, A. *J. Phys. Chem. B.* **1993**, *97*, 5430−5434.
(29) Baglioni, P.; Nakamura, H.; Kevan, L. *J. Phys. Chem.* **1991**, *95*, 5, 3856−3859.
(30) D'Aprano, A.; Lizzio, A.; Liveri, V. T.; Aliotta, F.; Vasi, C.; Migliardo, P. *J. Phys. Chem. B.* **1988**, *92*, 4436−4439.
(31) Boned, C.; Peyrelasse, J.; Mohaouchane, M. *J. Phys. Chem. B.* **1986**, *90*, 634−637.
(32) Day, R. A.; Robinson, B. H.; Julian H. R.; Clarke, J. H. R.; Doherty, J. V. *J. Chem. Soc., Faraday Trans. 1* **1979**, *75*, 132−139.

 10.1021/ja0624319 CCC: $33.50

Researchers have used various molecular probes to investigate properties of the RMs, such as microviscosity,[34,35] pH,[36] and polarity.[37] For example, measuring transient absorption of Auramine O, Hirose et al. found substantially slower rotational dynamics inside the RMs than in bulk solution.[34,35] Similarly, magnetic resonance studies of nitroxide probes such as TEMPO or TEMPAMINE show reduced rotational motion when confined in RMs.[38] Many different molecular probes have been used to gauge pH in RMs. From steady-state fluorescence and absorption spectroscopy of proton-donating molecules, pyranine and fluorescein, Hasegawa found that AOT headgroups appear to buffer the RM interior.[39] In another study, Biswas et al. showed that pH values at the interface of AOT RMs were greater than those at their cores using absorption and emission spectroscopy of 7-hydroxycoumarin and pyranine.[40] The chemical shift of inorganic phosphate can also be used to indicate the pH of a solution; Fujii et al. have used ^{31}P NMR spectroscopy to monitor environmental changes in RMs.[41,42] These experiments also suggest that the AOT surface buffers the intramicellar aqueous solution. In the work presented here, we utilize a charged inorganic polyoxovanadate, specifically decavanadate, as a probe for the RM water pool.

Vanadium(V) undergoes a range of protonation and oligomerization equilibria in aqueous solution.[43] The simple and colorless vanadate oligomers including vanadate monomer (V_1), dimer (V_2), tetramer (V_4), and pentamer (V_5) interchange with each other on the millisecond to second time scale in neutral and basic aqueous solution unlike the yellow-orange decavanadate (V_{10}), whose interconversion with the other oligomers occurs on a substantially longer time scale.[44] Decavanadate, V_{10} ($[V_{10}O_{28}]^{6-}$), whose structure is shown in Figure 1, is the thermodynamically stable oxovanadate species in aqueous solutions from pH 3 to 6.[45] Below pH 2, V_{10} rapidly hydrolyzes to VO_2^+; although not thermodynamically the most stable form above pH 6, V_{10} can persist for limited time periods because of its slow hydrolysis into other vanadate oligomers.[45] Three different types of vanadium atoms each bound to six oxygen atoms and in a slightly distorted environment comprise each V_{10} molecule. Four V_C atoms lie in an axial position, four V_B atoms are in the equatorial plane, and two V_A atoms lie at the center of the equatorial plane, as shown in Figure 1a.

Vanadium compounds are excellent probe of their surroundings due to the quadrupolar relaxation of vanadium in solution, along with the natural abundance (99.76%) and receptivity of

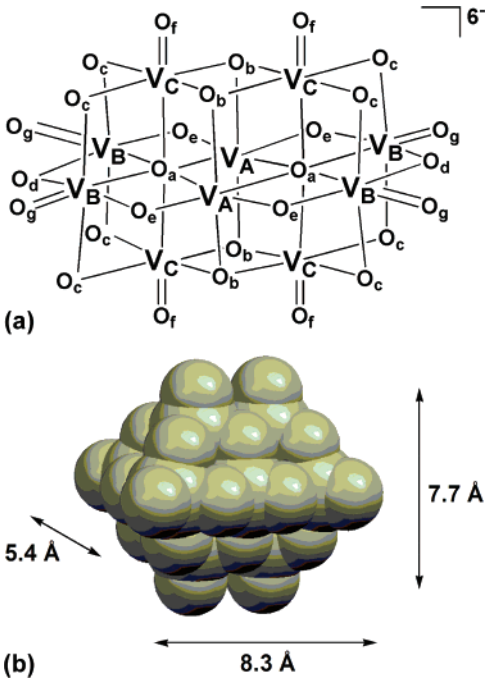

Figure 1. (a) Structure of $[V_{10}O_{28}]^{6-}$ (V_{10}). The three different types of V atoms are labeled V_A, V_B, and V_C. (b) Space-filled model of V_{10}.

the ^{51}V nucleus from its magnetic moment. ^{51}V NMR chemical shifts serve as excellent diagnostics to monitor small changes in the vanadium(V) coordination environment as they are very sensitive to changes in the electronic nature of the vanadium atom.[46−48] Therefore, ^{51}V NMR spectroscopy is a convenient method to monitor the speciation of oxovanadates. The distribution of and interaction between oligomers present in the ^{51}V NMR spectrum can reflect changes in solution pH and ionic strength.[43,45,46,49] At pH values from 3 to 6, V_{10} dominates the spectrum, and its changes in protonation states allow pH changes to be monitored. In its deprotonated form, V_{10} carries a −6 charge; it protonates as the pH drops below 6 as shown in eqs 1 to 3.[46]

$$V_{10}O_{28}^{6-} + H^+ \rightarrow HV_{10}O_{28}^{5-} \quad pK_1 = 5.5 - 6.0^{45} \quad (1)$$

$$HV_{10}O_{28}^{5-} + H^+ \rightarrow H_2V_{10}O_{28}^{4-} \quad pK_2 = 3.1 - 3.7^{45} \quad (2)$$

$$H_2V_{10}O_{28}^{4-} + H^+ \rightarrow H_3V_{10}O_{28}^{3-} \quad pK_3 \approx 2^{45} \quad (3)$$

At pH 3 the three different vanadium atoms in the trianionic V_{10} display ^{51}V NMR signals at −525, −507, and −424 ppm corresponding to V_C, V_B, and V_A, respectively. Successive deprotonation of the V_{10} anion leads to a downfield chemical shifts for the V_C and V_B ^{51}V NMR peaks to −516 and −500 ppm, respectively. This deprotonation has also been substantiated in detail by ^{17}O NMR studies.[50] Lifetime and line width measurements further report on the mobility of the probe. Combined, these properties indicate that V_{10} is an excellent

(33) Piletic, I. R.; Moilanen, D. E.; Spry, D. B.; Levinger, N. E.; Fayer, M. D. *J. Phys. Chem. A* **2006**, *110*, 4985−4999.
(34) Hasegawa, M.; Sugimura, T.; Suzaki, Y.; Shindo, Y.; Kitahara, A. *J. Phys. Chem.* **1994**, *98*, 2120−2124.
(35) Hirose, Y.; Yui, H.; Sawada, T. *J. Phys. Chem. B* **2004**, *108*, 9070−9076.
(36) Caselli, M.; Mangone, A.; Traini, A. *Ann. Chim.* **1998**, *88*, 299−318.
(37) Ueda, M.; Kimura, A.; Wakida, T.; Yoshimura, Y.; Schelly, Z. A. *J. Colloid Interface Sci.* **1994**, *163*, 515−516.
(38) Yushmanov, V. E.; Tabak, M. *J. Colloid Interface Sci.* **1997**, *191*, 384−390.
(39) Hasegawa, M. *Langmuir* **2001**, *17*, 1426−1431.
(40) Biswas, S.; Bhattacharya, S. C.; Bhowmik, B. B.; Moulik, S. P. *J. Colloid Interface Sci.* **2001**, *244*, 145−153.
(41) Fujii, H.; Kawai, T.; and Nishikawa, H. *Bull. Chem. Soc. Jpn.* **1979**, *52*, 2051−2055.
(42) Fujii, H.; Kawai, T.; Nishikawa, H.; Ebert, G. *Colloid. Polym. Sci.* **1982**, *260*, 697−701.
(43) Crans, D. C. *Comments Inorg. Chem.* **1994**, *16*, 1−33.
(44) Crans, D. C.; Rithner, C. D.; Theisen, L. A. *J. Am. Chem. Soc.* **1990**, *112*, 2901−2908.
(45) Howarth, O. W.; Jarrold, M. *J. Chem. Soc., Dalton Trans.* **1978**, 503−506.
(46) da Silva, J. L. F.; da Piedade, M. F. M.; Duarte, M. T. *Inorg. Chim. Acta* **2003**, *356*, 222−242.
(47) Gresser, M. J.; Tracey, A. S. *J. Am. Chem. Soc.* **1985**, *107*, 4215−4220.
(48) Heath, E.; Howarth, O. W. *J. Chem. Soc., Dalton Trans.* **1981**, 1105−1110.
(49) Baruah, B.; Crans, D. C.; Levinger, N. E. *Langmuir* **2006**. Manuscript in preparation.
(50) Klemperer, W. G.; Shum, W. *J. Am. Chem. Soc.* **1977**, *99*, 3544−3545.

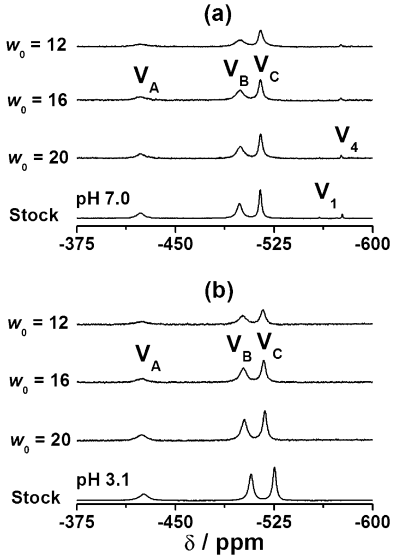

Figure 2. Representative ^{51}V NMR spectra of V_{10} (a) in stock 10 mM (100 mM V atoms) solution at pH 7.0 and inside reverse micelles created with pH 7.0 stock solution; (b) in 10 mM stock solution at pH 3.1 and inside reverse micelles created with pH 3.1 stock solution. The spectra were recorded at 78.9 MHz using ^{51}V NMR parameters described previously.[44,75]

spectroscopic probe to explore aqueous solutions, such as the RM interior.[51]

The work presented here utilizes V_{10} as a probe to explore the nature of the RM interior in large water/AOT/isooctane RMs with w_0 = 12, 16, and 20. The substantial and uniformly distributed negative charge on the V_{10} molecule should lead it to reside in the water pool away from the negatively charged headgroups of AOT RMs. Following the ^{51}V NMR of the intramicellar V_{10} allows us to measure properties of the micellar interior. While studies suggest that, in large RMs $w_0 > 10$, the amount and nature of water in the environment sampled by the V_{10} should be those of bulk water,[25−33] the results from the experiments reported here indicate otherwise. Results show that the influence of the RM interior leads to deprotonation of V_{10} introduced in an aqueous solution at pH 3 and that the microviscosity remains higher than that of bulk water.

II. Results

II. A. ^{51}V NMR Studies of V_{10} in Aqueous Solution and in RMs. Solution preparations are described in the figure captions of data shown, but more detailed experimental information is available in the Supporting Information. We measured the spectrum of V_{10} in RM samples generated using stock solutions ranging from pH 3.1 to 8.0. Figure 2 shows the ^{51}V NMR spectra obtained for V_{10} in RMs with w_0 = 12, 16, and 20, and the original stock solution. Three spectral features comprise the V_{10} spectrum; two peaks appear at −525.3 and −501.0 ppm in the pH 3.1 stock solution differing from those observed at pH 7.0, −514.3 and −498.3 ppm. These chemical shifts reflect the different protonation states of V_{10} present at the two pH values. In contrast, the spectra of V_{10} in the RMs remain surprisingly constant; neither pH nor w_0 appears to alter the chemical shifts. Figure 2 also shows substantial increases in line widths for the three V_{10} signals in the RMs.

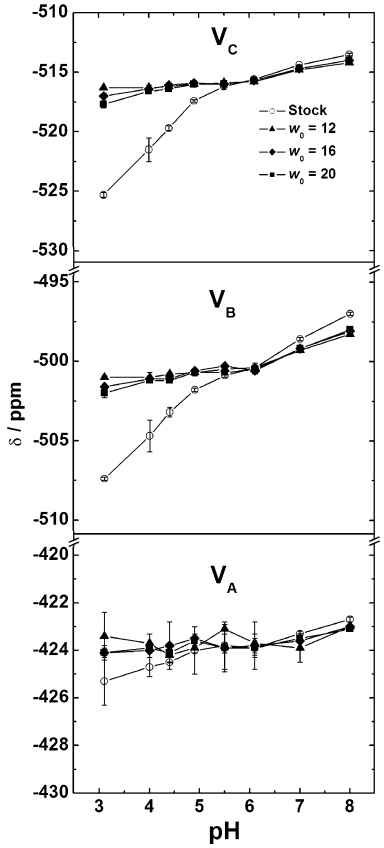

Figure 3. ^{51}V NMR chemical shifts as a function of pH for each vanadium atom type (V_C, V_B, and V_A) in V_{10}. Data were obtained using experimental detail referred to in the caption of Figure 2. Error bars indicate standard error (SE) on triplicate measurements; when none are visible symbols cover error bars.

Given the changes in the chemical shifts observed between pH 3.1 and 7.0 shown in Figure 2, we measured the spectra of V_{10} in RM samples as a function of stock solution pH from 3 to 8. Figure 3 shows the chemical shifts observed for the three different V atoms present in V_{10} as a function of the pH. The chemical shifts for V_{10} in the stock solution are also shown for comparison. The chemical shift of V_C (see Figure 1) in stock solution at pH 3 differs from the corresponding V_C in the RM by 8 ppm, while that for the V_B atom is nearly 6 ppm. In contrast, the chemical shift of V_A from the stock solution is conserved inside the AOT RM. Most likely because the V_A atom is deeply buried within V_{10}, its chemical shift is less sensitive to changes in the external environment. The line widths also change as the stock solution pH is varied (see Figure S1, Supporting Information).

To explore the impact of the RM environment, we present in Figure 4 the chemical shifts of the V atoms in the V_{10} molecule as a function of w_0 for RMs formed from V_{10} stock solutions at pH 3.1 and 7.0. The chemical shifts for the molecule in the aqueous stock solutions at the two bracketing pH values, 3.1 and 7.0, are shown for comparison. These plots reveal large differences in the chemical shifts for V_C and V_B inside the RMs compared to the stock solution at pH = 3.1 for all RM sizes probed. A gradual change in the chemical shift was observed for the entire w_0 range studied. While the chemical shifts observed differ little from one RM size to another when formed with a pH 7.0 stock solution, differences are observed with respect to the stock solution chemical shift for V_B and V_C. In

(51) Crans, D. C.; Rithner, C. D.; Baruah, B.; Gourley, B. L.; Levinger, N. E. *J. Am. Chem. Soc.* **2006**, *128*, 4437−4445.

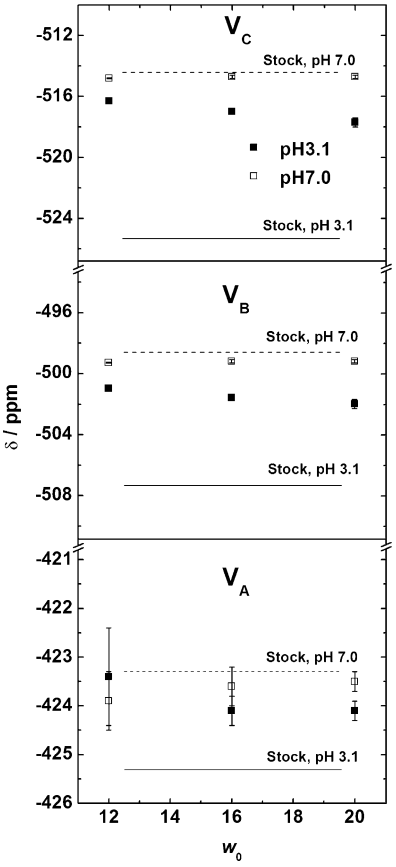

Figure 4. ^{51}V NMR chemical shifts obtained at 78.9 MHz as a function of w_0 in reverse micelles prepared from AOT (0.5 M)/isooctane and an aqueous 10 mM V_{10} stock solution at pH 3.1 (solid squares) and pH 7.0 (open squares) for each vanadium atom type (V_C, V_B, and V_A) in V_{10}. ^{51}V NMR chemical shifts for V_{10} in stock solution at pH 3.1 (solid line) and 7.0 (dashed line) are shown for comparison.

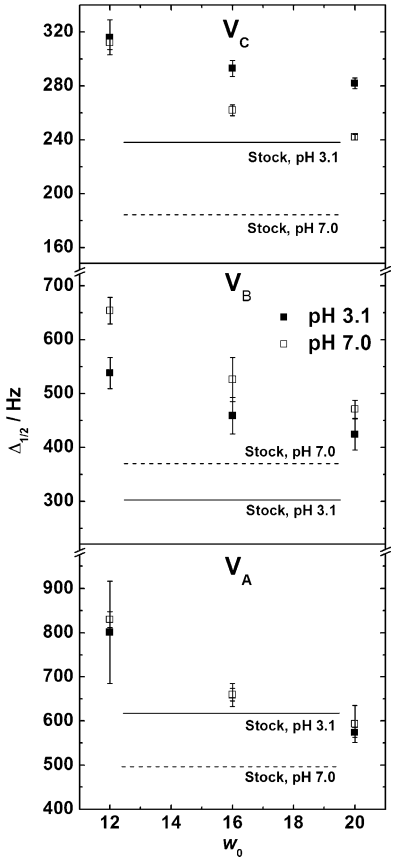

Figure 5. ^{51}V NMR line widths obtained at 78.9 MHz as a function of w_0 in reverse micelles prepared from an AOT (0.5 M)/isooctane and a 10 mM V_{10} stock solution at pH 3.1 (solid squares) and pH 7.0 (open squares) for each vanadium atom type (V_C, V_B, and V_A) in V_{10}. ^{51}V NMR line widths for V_{10} in stock solution at pH 3.1 (solid line) and 7.0 (dashed line) are shown for comparison.

RMs containing the pH 3.1 stock solution, the chemical shift is closer to the chemical shift in the stock solution in the larger RMs. However, even at $w_0 = 20$ the chemical shift is far from that of stock solution, suggesting that these environments are very different.

The line widths of the ^{51}V signals in the V_{10} molecule are shown in Figure 5 as a function of w_0 for RMs formed from pH 3.1 and 7.0 stock solutions. Changes in the line widths for V_B and V_C signals are greatest for the RMs prepared from the pH 7.0 stock solution. Specifically, spectral features of V_{10} in the stock solution broaden in RMs, with broader signals in smaller RMs. The increasing line width trend is greatest for V_A in the smallest RMs. Lifetime experiments were done, documenting that the observed changes are attributed to changes in molecular environment. While the line width decreases with increasing RM size, it never reaches the value of the stock solution as can be observed in plots of line width for V_C, V_B, and V_A as a function of w_0 shown in Figure 5. The ^{51}V NMR line widths also vary as a function of pH but show no clear trends (Figure S1, Supporting Information).

II. B. Dynamic Light-Scattering And Conductivity Experiments Characterizing the RMs Containing Water and V_{10}. Because addition of V_{10} to the microemulsion could change the characteristics of the solution,[52−56] we performed a range of experiments to explore the nature of the microemulsions, including dynamic light scattering, to compare the sizes of RMs containing water and V_{10} solution, as well as conductivity and viscosity measurements. The sizes of RMs could be measured with an overall AOT concentration of 0.2 M where the viscosity of the solution is close to that for isooctane. Data for these measurements are given in Table 1. Also given are the estimated numbers of V_{10} probe molecules present in the RMs. These data show that the size of the RMs varies within the error of the measurement. Thus, within the parameters of the experiments

Table 1. Reverse Micellar Properties: Radii for Reverse Micelles Containing Aqueous 10 mM V_{10} or Pure Water Measured Using Dynamic Light Scattering at a Viscosity of 0.691 cP and a Refractive Index of 1.391 Measured at 826.6 nm and at 25 °C, and Number of V_{10} Molecules per RM in the AOT (0.2 M)/Isooctane System

w_0	R_h/nm; V_{10} RMs[a]	R_h/nm; H_2O RMs[b]	n_{occ}[c]
12	3.6 ± 0.1	4.0 ± 0.1	3
16	4.0 ± 0.3	4.1 ± 0.1	6
20	4.2 ± 0.1	4.5 ± 0.2	11

[a] Stock solution pH = 6.0 [b] Stock solution pH = 5.7 [c] Estimated from the reverse micelle aggregation number[57] and overall vanadate concentration.

(52) Maitra, A. *J. Phys. Chem.* **1984**, *88*, 5122−5125.
(53) Bohidar, H. B.; Behboudnia, M. *Colloids Surf., A* **2001**, *178*, 313−323.
(54) Zulauf, M.; Eicke, H.-F. *J. Phys. Chem.* **1979**, *83*, 480−486.
(55) Andrews, B. A.; Pyle, D. L.; Asenjo, J. A. *Biotechnol. Bioeng.* **1994**, *43*, 1052−1058.
(56) Spirin, M. G.; Brichkin, S. B.; Razumov, V. F. *Zh. Nauchn. Prikl. Fotogr.* **2000**, *45*, 20−27.

performed here, our results show that the RMs are not perturbed by dissolution of the V_{10} molecule.

Electrical conductivity of the RM system was also used to compare RMs containing water and V_{10} solutions. The conductivity of water-in-oil microemulsions in RMs containing water shows variations over many orders of magnitude as the phase changes.[58,59] The conductivity of RMs encapsulating V_{10} prepared from 0.5 M AOT stock solution was 0.4 μS cm^{-1}. Corresponding RMs prepared with 0.5 M AOT stock solution and pure water show the same conductivity. Similarly, the electrical conductivity of RM solutions prepared from 0.2 M AOT is 0.1 μS cm^{-1} whether pure water or aqueous V_{10} forms the interior. In contrast, the electrical conductivity of the 100 mM $NaVO_3$ aqueous stock solution is significantly higher, 8.7 mS cm^{-1}.

The studies described above were all obtained for RMs formed in 0.5 M AOT solutions that show somewhat increased conductivity compared to lower AOT concentrations. Our previous work suggests that at 0.5 M AOT in isooctane, RMs tend to aggregate or flocculate.[51] Thus, we explored the impact of AOT concentration to learn what effect, if any, the RM concentration has on the observed ^{51}V NMR signals. Upon dilution of the AOT to 0.2 M, similar ^{51}V NMR experiments yielded results indistinguishable from those carried out at the higher AOT concentration. The only differences observed were the change of vanadate oligomer speciation toward the neutral pH and the poorer signal-to-noise resulting from lower overall concentration of V_{10}. Therefore, although the RMs may aggregate or flocculate in 0.5 M solutions, the environment of the V_{10} species is conserved. These results indicate that incorporation of V_{10} in the RMs does not substantially perturb the RM structure.

III. Discussion

In AOT RMs, water molecules near the interface can solvate AOT headgroups, Na^+ counterions, or they can interact with other water molecules. Thus, it is not surprising that results from a wide range of experiments show that water near interfaces behaves differently than it does in bulk solution.[17,23,24,33,60−66] Water molecules perturbed by interactions with AOT and bulk-like water equilibrate continuously as molecules move from interface to core and back. However, in large RMs, $w_0 > 10$ or more generally when the water pool radius exceeds 22 Å, the intramicellar water is reported to develop characteristics similar to those of bulk water that can dominate the results observed.[25−33] Thus, in experiments utilizing large ($w_0 > 10$) RMs, the water often displays properties similar or identical to those observed in bulk solution. When results diverge from bulk water characteristics, researchers generally suggest that the molecular probes utilized must reside near the RM interface.[67] The results reported in this paper show that, even in the "bulk-like" water pools found in large RMs, RM water properties can differ substantially from those of bulk water.

All experiments reported here have been performed on RMs with $w_0 > 10$, when the RMs are large enough to support a bulk-like water pool. The large charge of the V_{10} molecule and its V−O bonds make this molecule very hydrophilic. That, combined with Coulombic repulsion between the substantial negative charge on V_{10} (between −6 and −4) and the negatively charged AOT headgroups, should drive the V_{10} into the RM water pool. The possibility still exists that V_{10} interferes with the formation and nature of the RMs, and the presence of the V_{10} molecule in the RM interior could itself influence the environment. On the basis of its size, we estimate that one V_{10} molecule takes up the same amount of volume as approximately 11−12 water molecules. Given that there are thousands of water molecules inside these RMs, it seems unlikely that removing 11 water molecules per V_{10} should strongly perturb the system. We explored the impact of V_{10} on RM formation and character using dynamic light-scattering experiments and conductivity. Dynamic light scattering experiments showed that the hydrodynamic radii of RMs and polydispersity for RMs with $w_0 =$ 12, 16, and 20 formed with water or aqueous stock solutions of V_{10} are the same (Table 1). This indicates that solubilization of the V_{10} molecule in the RMs changes neither their size nor their shape. Furthermore, RMs formed with pure water or aqueous V_{10} stock solution over the range of pH values show similar conductivity, 0.4 μS cm^{-1} and 0.1 μS cm^{-1}, at 0.5 and 0.2 M AOT, respectively. At concentrations above 0.2 M AOT the RMs flocculate, but ^{51}V NMR experiments suggest that the environment of V_{10} remains similar for 0.5 and 0.2 M AOT concentration. Electrical conductivity measurements show that addition of V_{10} in the water pool does not change the microemulsion phase. These results leave us confident that the V_{10} molecule does not interfere with RM formation or character and that it does not insert into the RM interface as we have observed for other vanadium-containing probes.[51]

The location of the V_{10} molecule in the RM should influence the observed ^{51}V NMR signal. Indeed, there is substantial evidence that the environment near the micellar interface differs significantly from the micellar core.[21,23,24,68] Sampling the interfacial region should lead the V_{10} molecule to report on water with properties different from bulk. At higher water content, $w_0 > 10$, the interfacial properties in AOT RMs formed in aliphatic hydrocarbon solvents, such as isooctane in the studies discussed here, become independent of water content.[17,68,69] Molecular probes sensing microviscosity or micropolarity that reside at the RM interface show significant variations with increasing RM size but approach a constant value for larger RMs. While Coulombic repulsion is not always sufficient to determine molecule location in a RM,[51,70] the continuing changes

(57) Chowdhury, P. K.; Ashby, K. D.; Dutta, A.; and Petrich, J. W. *Photochem. Photobiol.* **2000**, *72*, 612−618.
(58) Tsao, H. K.; Sheng, Y. J.; Lu, C. Y. D. *J. Chem. Phys.* **2000**, *113*, 10304−10312.
(59) Liu, D.; Ma, J.; Cheng, H.; Zhao, Z. *Colloids Surf., A* **1998**, *135*, 157−164.
(60) Benderskii, A. V.; Henzie, J.; Basu, S.; Shang, X. M.; Eisenthal, K. B. *J. Phys. Chem. B* **2004**, *108*, 14017−14024.
(61) Bhide, S. Y.; Berkowitz, M. L. *J. Chem. Phys.* **2005**, *123*.
(62) Grant, C. D.; Steege, K. E.; Bunagan, M. R.; Castner, E. W. *J. Phys. Chem. B* **2005**, *109*, 22273−22284.
(63) Harpham, M. R.; Ladanyi, B. M.; Levinger, N. E.; Herwig, K. W. *J. Chem. Phys.* **2004**, *121*, 7855−7868.
(64) Kotake, Y.; Janzen, E. G. *J. Phys. Chem.* **1988**, *92*, 6357−6359.
(65) Levinger, N. E.; Riter, R. E. In *Liquid Interfaces in Chemical, Biological, and Pharmaceutical Applications*; Volkov, A. G., Ed.; Marcel Dekker: New York, 2001; pp 399−413.
(66) Schwartz, L. J.; DeCiantis, C. L.; Chapman, S.; Kelley, B. K.; Hornak, J. P. *Langmuir* **1999**, *15*, 5461−5466.
(67) Hunt, N. T.; Jaye, A. A.; Meech, S. R. *Chem. Phys. Lett.* **2005**, *416*, 89−93.
(68) Correa, N. M.; Biasutti, M. A.; Silber, J. J. *J. Colloid Interface Sci.* **1995**, *172*, 71−76.
(69) Silber, J. J.; Biasutti, A.; Abuin, E.; Lissi, E. *Adv. Colloid Interface Sci.* **1999**, *82*, 189−252.
(70) Stover, J.; Rithner, C. D.; Inafuku, R. A.; Crans, D. C.; Levinger, N. E. *Langmuir* **2005**, *21*, 6250−6258.

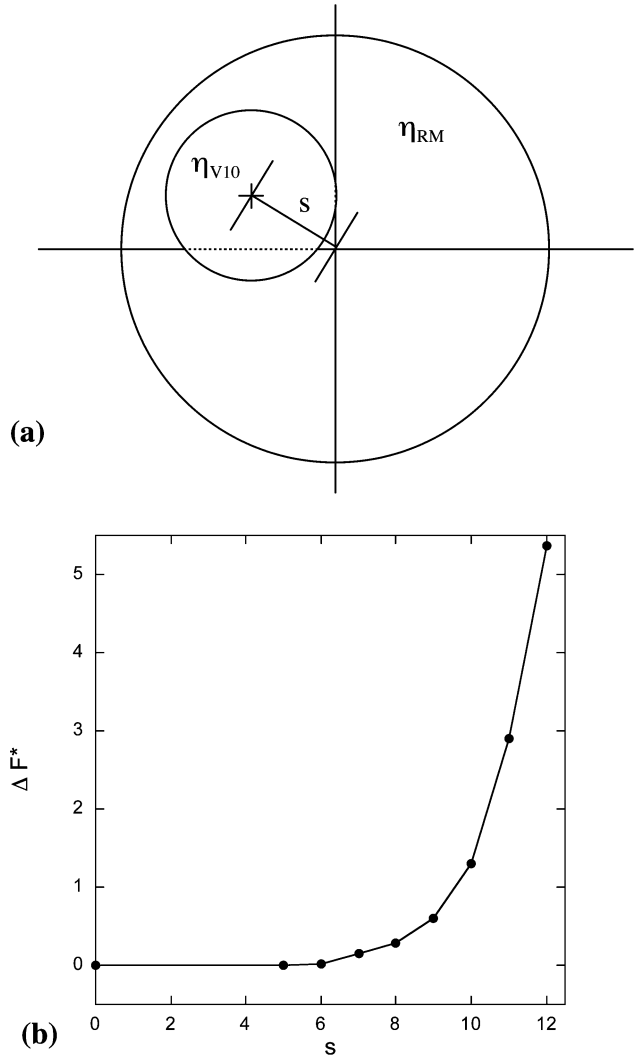

Figure 6. (a) Geometric depiction of the location of the V_{10} complex in a reverse micelle corresponding to parameters from eqs 4−8. (b) Free energy as a function of intercenter distance, *s*, as described in the text. Parameters for graph are as follows, $R_{V10} = 7$, $R_{RMs} = 75$, V_{10} charge $= -6$, and RMs charge is set to -1.

in chemical shifts and line widths (Figures 4 and 5) that we observe suggest V_{10} does not remain solvated at the RM inner interface and rather resides in the core water pool. In addition, we note that in small AOT RMs, dramatic changes to ^{51}V NMR signals are apparently consistent with the V_{10} molecule approaching and interacting with the interface. (We have measured ^{51}V NMR spectra for V_{10} in AOT RMs with $w_0 < 10$. In these systems, we observe unequal influence on the peaks in the NMR spectra as V_B and V_C atoms interact more strongly with the interface. These data will be published in a forthcoming paper.)

Because the V_{10} molecule carries a significant negative charge and the RM interface is also charged, the simple model system of two charged, eccentric spheres developed by Sengupta and Papadopoulos[71] can be used to model the V_{10} in the RMs. This model places a rigid, solid, inner sphere, that is, the V_{10} molecule, inside a hollow, rigid, outer sphere, the RM, as depicted in Figure 6a. No shape fluctuations are permitted for either sphere. While the form of the V_{10} molecule is not perfectly spherical, as shown in Figure 1b, a spherical form with uniform charge density is a reasonable first approximation. The V_{10} (inner sphere) is allowed to move radially from the RM (outer sphere) center to the interface; the displacement of RM and V_{10} centers is given by distance *s*. Then using the Poisson−Boltzmann equation to determine the electric potential, Ψ, eq 4,

$$\nabla^2\Psi = \frac{8\pi nez}{\epsilon}\sinh\frac{ze\Psi}{kT} \tag{4}$$

where n is the number concentration of ions in the bulk, e is the charge of the electron, z is the valency of ions, ϵ is the dielectric constant of the electrolyte, k is the Boltzmann constant, and T is the temperature, we calculate the free energy of interaction between the V_{10} and the RM,[72]

$$\Delta F = F_{sys} - \sum_{i=1}^{2} F_i \tag{5}$$

where

$$F_{tot} = -\frac{\epsilon}{8\pi}\int\int\int_{\nu}|\nabla^2\Psi|^2\,dV - 2nkT\int\int\int_{\nu}\left(\cosh\frac{ze\Psi}{kT} - 1\right)dV \tag{6}$$

F_{tot} can be simplified and made dimensionless by the substitution

$$F^*_{tot} = \frac{F_{tot}\kappa^3}{nkT} \tag{7}$$

where

$$\kappa^2 = \frac{8\pi ne^2z^2}{\epsilon kT} \tag{8}$$

Here F_{sys} is the energy when the surfaces of the spheres interact, and F_i is the energy when the spheres have no interactions. To compute ΔF requires the free energies of the individual spheres that depend on a few parameters, such as surface charge and sphere radii that we estimate from data about AOT RMs and the V_{10}.[73] This allows ΔF^* to be determined as a function of the separation distance of the sphere centers, *s*, defined in Figure 6a. (We made a few simplifying assumptions to compute ΔF^*. Applying the Poisson−Boltzmann equation assumes a symmetric electrolyte solution, which does not model the RM interior perfectly. However, the calculation is valid as long as the density of ions at the interfaces remains fixed.[74] In addition, as the dielectric constant of the particle is smaller than that of the electrolyte solution, the overall result is a constant Debye length, κ, leading to overall scaling by κ.[75]) While a uniform charge density is assumed for each sphere, when we varied the charges on the inner and outer spheres over a wide range of values, we obtained comparable results.

Figure 6b shows ΔF^*, the dimensionless interaction energy, as a function of the separation distance. At $s = 0$, the V_{10} resides at the center of the RM; $s = 12$ places V_{10} at the interface. For plots shown in Figure 6b, we assume that the V_{10} radius is 9.3%

(71) Sengupta, A. K.; Papadopoulos, K. D. *J. Colloid Interface Sci.* **1992**, *149*, 135−152.
(72) Verwey, E. J. W.; Deboer, F.; Vansanten, J. H. *J. Chem. Phys.* **1948**, *16*, 1091−1092.
(73) Evans, H. T., Jr. *Inorg. Chem.* **1966**, *5*, 967−977.
(74) Levine, S. *Proc. Phys. Soc.* **1951**, *64*, 781−790.
(75) Hsu, J.-P.; Kao, C.-Y. *Langmuir* **2002**, *18*, 2743−2749.

of the RM radius, on the basis of the V_{10} crystal structure[73] and a RM with $w_0 = 12$. Varying the RM size from 12 to 20 led to changes too small to observe. Variation of the interfacial charge between -1 and -2, corresponding to the anticipated number of AOT headgroups with which the V_{10} complex interacts, leads to very minor differences in ΔF or ΔF^*.

V_{10} sequestered in the AOT RM allows us to compare different parameters and how they affect the interaction of V_{10} at the interface. The plot shown in Figure 6b indicates that the free energy increases with increasing *s*, which suggests that if Coulombic interactions dominate the placement, the V_{10} should reside preferentially away from the micellar interface. Only if the V_{10} possesses an asymmetric charge distribution or if its size approaches the size of the interfacial cavity can it reside near or in the interfacial layer. On the basis of data about V_{10}[73] and the protonation state we measure with NMR, the V_{10} complex should possess a symmetric charge distribution therefore placing it in the RM water pool and not at the interface.

Both literature precedent[69,71] and our calculations indicate that the large, negatively charged V_{10} ($[V_{10}O_{28}]^{6-}$) molecule should reside away from the interface where it would probe a bulk-like water environment. Preference for this location should be greater the greater the charge of the V_{10} molecule. Varying the pH of the stock solution from 3 to 8 results in a net change from -6 to -4 on the V_{10} molecule. Thus, one might expect these experiments to yield spectra similar or identical to those measured in bulk aqueous solution, but the data indicate otherwise.

The V_{10} signals both shift downfield, and the line widths narrow as the water content w_0 increases. However, neither chemical shift nor line width in any of the systems at any starting pH value achieves the corresponding values we observe for the molecule in bulk solution (Figures 4 and 5). Many studies reported in the literature indicate that a bulk-like water pool should have developed at $w_0 > 10$.[25−32] The continuing changes we observe as w_0 increases from 12 to 20 and the fact that the bulk values are never reached show that the V_{10} environment in all the RMs studied differs from that of bulk water and continues to change in these systems. Thus, we believe that it is the water that has not reached its bulk limit rather than a strong perturbation of the vanadium stock solution on the water. The fact that the chemical shifts and the line widths continue to change above this hydration level suggests that the free water pool has still not achieved bulk-like character with respect to the V_{10} environment. Thus, if the intramicellar water pool has the properties of bulk water, then the V_{10} NMR signals should reflect these water pool properties and should display, at most, minor differences from those observed in bulk solution.

The chemical shifts of the surface-exposed sites V_C and V_B in RMs differ dramatically from those observed for V_{10} in aqueous solution, especially for low pH stock solutions. The chemical shifts of protonated V_{10} in aqueous stock solution at pH 3.1 are -525.3 (V_C), -507.4 (V_B), and -425.3 (V_A), whereas the chemical shifts of this solution added to the RMs appear at -517.0 (V_C), -501.6 (V_B), and -424.1 (V_A). Given its sensitivity to protonation,[47,48] the ^{51}V chemical shift of V_{10} can be used to probe the local pH of environment inside the RMs. The chemical shift differences for V_C and V_B are consistent with deprotonation of V_{10} in bulk solution.[48] This observation suggests that proton concentration in the environment sensed by V_{10} in the RMs is lower than that of the stock solution from which the RMs were formed. Interestingly, the chemical shifts we observe for V_{10} inside the RMs appear conserved regardless of the protonation state in the stock solution (Figures 2 and 3, Table S1, Supporting Information).

The smallest changes in chemical shift and line width are observed for the V_A atom in the V_{10} molecule (Figures 3 and 5). This nonoxovanadium atom differs significantly from the surface-exposed V_B and V_C atoms. The chemical shift for V_A is similar in RMs and in bulk solution at all pH values. Completely surrounded by oxygen and other vanadium atoms, its environment isolates V_A from the exterior, rendering it far less sensitive to changes in the environment. Thus, this vanadium serves as an excellent internal reference for this probe. In other words, changes observed for V_B and V_C but not for the V_A atom reflect surface-type interactions of V_B and V_C.

The conundrum arises, why does the V_{10} molecule report different proton concentration in the RM interior than the starting stock solution? The significant charge on the V_{10} molecule should lead it to reside well solvated by many intramicellar water molecules while sodium counterions balance both the charge of the V_{10} and the AOT sulfonate headgroups. However, the ^{51}V NMR chemical shifts indicate that the RM interior differs substantially from the original stock solution. An inhomogeneous electrical potential can arise inside the RM when counterions dissociate from the interfacial region.[76] A theoretical calculation shows a significant decrease in the potential, increasing the dielectric constant of the media as w_0 increases which could determine the distribution of charged species inside the RMs.[76,77] Recent calculations modeling ion exchange inside the RM show that if the diameter of an added cation is greater than the Na^+ counterion diameter, the cation migrates toward the headgroup region of the RM.[76] As protons aggregate to H_3O^+ and larger aggregates in water,[78−80] their size exceeds the Na^+ and should lead H^+ to migrate preferentially to the interface while Na^+ migrates to the micellar interior as depicted in Figure 7. This migration leads to a proton gradient inside the RM giving rise to different apparent pH values in the interface and in the central water pool. Thus, a complex like V_{10} located in the water pool of the RM senses a proton concentration that is substantially different than that of the water in the interface or in the original stock solution. Specifically, a symmetrical probe located in the water pool will report a local pH more basic than the original acidic stock solution used for preparation of the RMs. As w_0 increases, the dielectric potential drops, resulting in a proton migration to the interface, rendering the water pool slightly more acidic than at lower w_0.

The observation that V_{10} yields the same ^{51}V NMR chemical shifts when added to the RMs regardless of the pH of the initial stock solution can be interpreted as the RMs having a buffering effect on the water pool. Our observation that the chemical shifts change toward the values in the bulk stock solution with increasing w_0 increases at a fixed pH supports this interpretation.

(76) Pal, S.; Vishal, G.; Gandhi, K. S.; Ayappa, K. G. *Langmuir* **2005**, *21*, 767−778.
(77) Tomic, M.; Kallay, N. *J. Phys. Chem.* **1992**, *96*, 3874−3882.
(78) Voth, G. A. *Acc. Chem. Res.* **2006**, *39*, 143−150.
(79) Botti, A.; Bruni, F.; Imberti, S.; Ricci, M. A.; Soper, A. K. *J. Chem. Phys.* **2004**, *121*, 7840−7848.
(80) Marx, D.; Tuckerman, M. E.; Hutter, J.; Parrinello, M. *Nature* **1999**, *397*, 601−604.
(81) Zhang, J.; Bright, F. V. *J. Phys. Chem.* **1991**, *95*, 7900−7907.

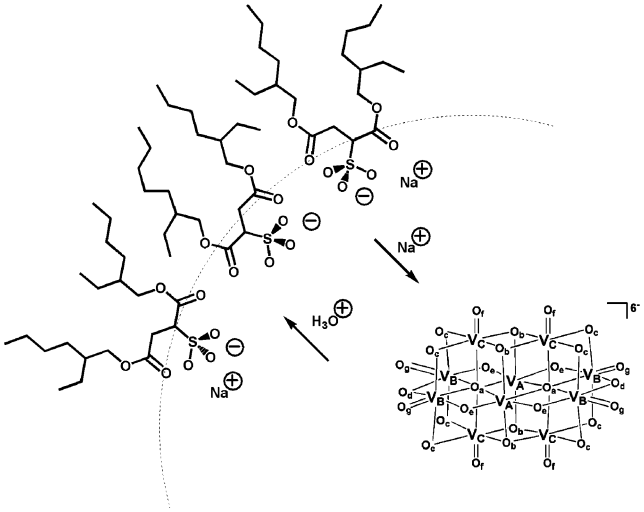

Figure 7. Schematic depiction of the location of V_{10} with respect to the reverse micellar interface including counterions.

The possibility that the water pool of the RMs is buffered has previously been suggested on the basis of studies carried out with emission spectroscopy.[35,39] The buffering capacity of the water pool in *n*-heptane/AOT/water RMs was related to the considerably high AOT sulfonate concentration localized at the interface of the aggregate.

The chemical shifts observed for the V_B and V_C atoms in V_{10} show almost no dependence on the pH of the stock solution used to create the RMs, Figure 3. However, the line width changes as a function of pH (Table S2 and Figure S1, Supporting Information) consistent with changes in microfluidity in the RM interior. Microviscosity has been found to vary with the value of w_0.[34,81] In small RMs and low w_0, the water molecules hydrate the polar headgroup of the interface and the accompanying counterions. The key hydrogen bond structure present in the bulk water is destroyed when water interacts with the polar head of the surfactant. Only above $w_0 = 10$ when the interface has obtained the water molecules needed to complete the hydration sphere will the water molecules begin to form a water pool with characteristics of the "free" bulk-phase water, as determined by properties such as microviscosity and micropolarity.[37,40,68,82] The bound water found at interfaces at very small w_0, shows a very high microviscosity, and low polarity yields a very rigid interface. As the size of the RM increases the water content and w_0 increases, the microviscosity and, hence, the rigidity of the RM decrease.[37,40,68,82−84] Thus, the water pool and the interface of the RM are decreased in viscosity and increased in mobility as the w_0 increases. Since the line widths for two out of three V signals decrease with increasing w_0, the complex must sense a less viscous environment as the water content increases. However, it never reaches the value found in bulk water. This result is contrary to the many reports that characterize the water in RMs with $w_0 > 10$ as bulk water,[52] and suggests that, although by many criteria one would characterize the water as similar to bulk water, these studies show that other properties exist for which the water inside the RM is different than bulk water.

IV. Conclusions

The highly charged inorganic decavanadate anion (V_{10}) is used to probe the water environment in RMs formed by AOT in isooctane. The versatile inorganic probe utilized here, that is V_{10}, provides several spectroscopic handles that allow us to probe more than one property of AOT RMs at a time. Due to the large negative charge on V_{10} and the negatively charged surfactant headgroups, it is generally presumed that V_{10} would reside in the RM water pool. Continuing but small changes in the ^{51}V NMR chemical shifts and line widths with growing RM size confirm this presumption.

The V_{10} molecule is an effective and unique probe that allows us to measure two very important properties of the intramicellar water pool, that is proton concentration, or local pH, and microviscosity. The results presented here show that, despite sequestering large amounts of water within, the water in these RMs never reaches the values found for bulk water. Furthermore, the V_{10} molecule shows that the core region of the RMs remains at an apparent pH near neutral. Protons migrate toward the RM interfacial region, leaving the core region with counterions but no excess protons. These results could have tremendous impact for chemical reactions occurring in RMs, such as acid-catalyzed reactions, or biochemical reactions, as enzymatic reactions. While it is not clear that the nature of confined water pools share similarities with the AOT RMs, if they do, the implications could be far reaching for a wide range of processes occurring in confined environments.

Acknowledgment. This material is based upon work supported by the National Science Foundation under Grants No. 0314719 and 0244181. J.M.R. performed research under the auspices of the NSF REU program. N.M.C. holds a research position at CONICET and thanks the Fulbright Commission for the Research Award obtained in support of travel to Colorado State University, Fort Collins, CO.

Supporting Information Available: Experimental details. This material is available free of charge via the Internet at http://pubs.acs.org.

JA0624319

(82) Karukstis, K. K.; Frazier, A. A.; Martula, D. S.; Whiles, J. A. *J. Phys. Chem.* **1996**, *100*, 11133−11138.
(83) Wittouck, N.; Negri, R. M.; Ameloot, M.; Deschryver, F. C. *J. Am. Chem. Soc.* **1994**, *116*, 10601−10611.
(84) Wong, M.; Thomas, J. K.; Gratzel, M. *J. Am. Chem. Soc.* **1976**, *98*, 2391−2397.